^{19}F NMR studies of fluoride graphite intercalated compounds prepared under fluorine atmospheres

M. F. Quinton, S. Leonardelli, A. P. Legrand
Laboratoire de Physique Quantique, URA 421, ESPCI, 75231 Paris Cedex 05 (France)

R. Yazami
Laboratoire d'Ionique et d'Electrochimie du Solide de Grenoble, URA D 1213, ENSEEG, Domaine Universitaire BP 75, 38402 Saint Martin d'Hères (France)

and T. Nakajima
Division of Molecular Engineering, Graduate School of Engineering, Kyoto University, Sakyo-ku, Kyoto 606 (Japan)

Abstract

Fluorine nuclear magnetic resonance studies have been made on Group V (Sb, As) fluoride and metal (Ti, V) fluoride/antimony fluoride graphite intercalated compounds prepared under a fluorine atmosphere. All samples studied were made from highly oriented pyrolytic graphite. It is shown that in the Group V fluoride compounds, the fluoride is preferentially intercalated as $[MF_6]^-$ In metal fluoride/antimony fluoride compounds, the ^{19}F NMR spectra are consistent with antimony fluoride preferentially intercalated as $[SbF_6]^-$ in the vanadium compound, and as $[Sb_nF_{5n+1}]^-$ polyanions in the titanium compound. This latter result can be explained by the ability of titanium fluoride to form polymer chains, unlike vanadium fluoride No metal fluoride was observed in the latter systems.

Introduction

Synthesis of fluoride graphite intercalation compounds (GICs) under fluorine atmosphere leads to compounds where the intercalated species are highly fluorinated [1–3]. Particularly, in the case of arsenic and antimony fluoride GICs, first stage compounds having composition $C_{\approx 10}MF_6$ (M = As, Sb) have been obtained [3], in contrast to the other preparative methods [4, 5] where the composition is $C_{7\text{-}10}MF_5$. For the latter compounds, the charge transfer taking place between the graphite host and the fluoride guest involves the reaction:

$$2xC + 3MF_5 \rightleftharpoons C_{2x}{}^{2+}[MF_6]_2{}^-MF_3$$

Thus, in the final product, MF_3 was reported to appear as an inclusion (inside or outside the graphitic layers).

Fluoride/fluoride and fluoride/sulfuric acid graphite bi-intercalation compounds (GBCs) have also been prepared using this method [3]. Their synthesis was realized in two successive steps. First, a binary second-

0022-1139/92/$5.00

stage metallic fluoride GIC was prepared. Subsequent intercalation of a second fluorinated species was performed in such a way that the host GIC remained chemically stable.

X-ray diffraction analysis performed on the so-prepared GBCs was consistent with a model of regular stacking along the *c*-axis in the sequence G/A/G/B/G/A . . (G = graphitic layer, A and B = fluorinated species). This behaviour contrasts with that of ternary GICs where A and B are intimately mixed within the layers, and of co-intercalated GICs where no regular stacking of the two intercalates is observed.

To obtain more precise information about intercalated species in the compounds prepared under fluorine atmospheres, we performed a ^{19}F NMR of first-stage binary Group V fluorides GICs and metallic fluoride/antimony fluoride GBCs.

Experimental

Sample preparation

We restricted our ^{19}F NMR investigations to samples prepared from highly oriented pyrolytic graphite, spectra being easier to exploit in this case. Details on preparative conditions of binary GICs and GBCs have been published elsewhere [3], and for the studied samples are summarized in Tables 1 and 2 respectively. Also displayed are the chemical composi-

TABLE 1

Preparative conditions for binary fluoride GICs

Compound	Stage	T (°C)	P_{F_2} (atm)	Time (h)	Composition[1]		I_c (Å)
					x	y	
Ti–F	2	165	0.75	115	25.8	5.5	11.33
V–F	2	200	1	24	15.4	6	11.87
Sb–F	1	80	1	24	9.35	6	8.14
As–F	1	20	1	50	10.1	6	7.95

[1]Expressed by the chemical formula $C_x MF_y$

TABLE 2

Preparative conditions of metal fluoride/antimony fluoride GBCs

Binary metal fluoride	T (°C)	P_{F_2} (atm)	Time (h)	SbF_6 amount z[a]	I_c (Å)
$C_{25.8}TiF_{5.5}$	80	1	168	1.75	16.23
$C_{15.1}VF_6$	80	1	168	1.12	16.56

[1]Expressed by the chemical formula $C_x MF_y (SbF_6)_z$

tions of the samples, expressed as C_xMF_y for GICs and $C_xMF_y(M'F_6)_z$ for GBCs, and the identity period value I_c along the c-axis. It should be noted that except for stage 2 GIC with TiF_y, where the fluorine pressure was fixed at 0.75 atm to avoid the formation of stage 1 GIC, all other preparations were performed under 1 atm of fluorine. After the reaction, the samples were carefully transferred from the reactor to a glove box filled with dry argon, where they were stored. For NMR experiments, the samples were put into a rectangular glass tube using fibre-glass to prevent sample motion inside the tube. This tube was sealed outside the glove box.

NMR measurements

Our investigations were restricted to recording spectra at three main sample orientations: the sample c-axis parallel to, perpendicular to, and making the magic angle with the magnetic field B_0. At this last orientation, the anisotropic part of the interactions having axial symmetry around the sample c-axis is zero, making lineshape analysis easier. We will refer later to these orientations as $\Theta = 0°$, $\Theta = 90°$ and $\Theta = \Theta_m$ respectively.

^{19}F NMR spectra were obtained using a high field ($B_0 = 7T$) high power Bruker CXP 300 spectrometer at room temperature. An ASPECT 2000 computer was used to accumulate signals and to carry out data-processing. We used a Bruker ^{19}F probe with solenoid coil, slightly modified to remove the probe background signal. Sample orientation with respect to magnetic field was set up manually, and the accuracy of the sample position was estimated to be better than $\pm 2.5°$.

The spectra were recorded using a single-pulse sequence with phase cycling. The pulse duration was 1.5 μs or 2 μs, roughly corresponding to $\pi/2$ pulse. The free induction decay (FID) was recorded after 4 μs dead time, depending on the chosen frequency sweep width (125 kHz or 500 kHz), and using a 4 s repetition rate.

In the case of spectra with short dead time (500 kHz sweep width), the beginning of the FID is generally perturbed by the damping signal of the radiofrequency pulse. Thus before performing Fourier transform, the four first points of the signal were rectified, their correct positions being estimated by visual inspection of the FID shape according to the next points. Due to the good signal-to-noise ratio, it was not necessary to do any exponential multiplication before Fourier transformation. After zero-order phase correction, a slight baseline correction was applied.

To analyse lineshift, we used the so-called PASCAL FITLIN program running the ASPECT 2000 computer, which is a slightly modified version of the LINEFIT program from the ASPECT 2000 program library.

The ^{19}F shifts were measured with respect to C_6F_6 external reference. To allow comparison with other results, their values are reported with respect to $CFCl_3$, according to the standard convention which denotes negative (positive) shifts in the upfield (downfield) region ($\delta_{CFCl_3} = \delta_{C_6F_6} - 163$ ppm). All the spectra exhibit a very narrow line at -2.5 ppm which is

not due to the samples but to SiF_4 resulting from the reaction of desorbed fluorine with glass. Indeed, we observed with some samples in which this line disappears almost completely after removing the glass fibers used to keep the sample in position inside the NMR tube.

^{19}F NMR spectra of binary fluoride compounds

Results

The ^{19}F NMR spectra of the first stage antimony fluoride–graphite sample were presented in a previous paper [6]. To make easier comparisons with GBCs, the results are recalled here and the spectra are displayed in Fig. 1. The evolution of the spectra with the sample orientation is explained by the superposition of several lines, the width and shift of which are orientation-dependent

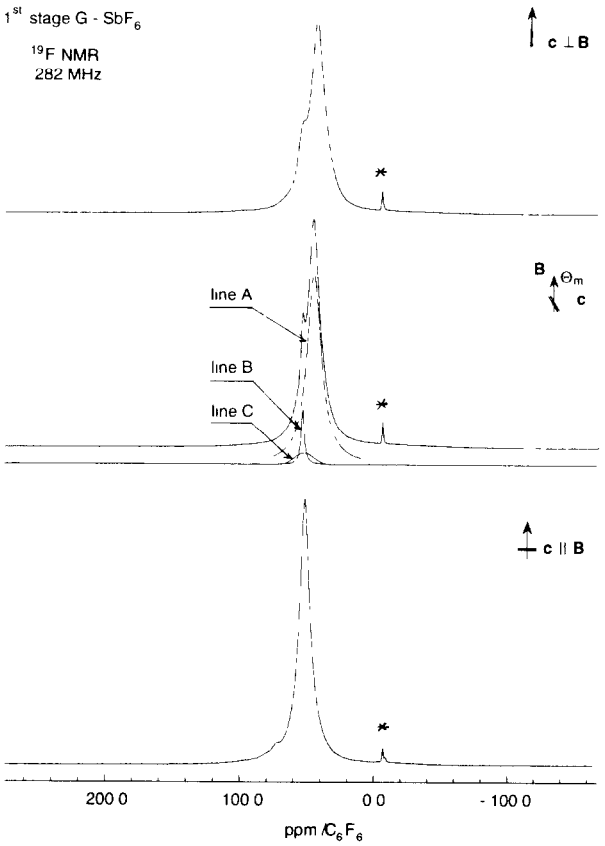

Fig 1 ^{19}F NMR spectra at room temperature of first stage binary SbF_6–GIC, at the three main sample orientations with respect to magnetic field (The line marked * is due to SiF_4, resulting from the reaction of desorbed fluorine with glass, see text)

We can distinguish unambiguously two lorentzian shape lines the shift of which is axially symmetric around the sample c-axis. The main line (A), which is representative of about 90% of fluorine atoms, has an isotropic shift of 45 ± 1 ppm, and its anisotropic shift (defined as $\delta_{\parallel} - \delta_{\perp}$) is positive. The other lorentzian line ($B \approx 5\%$ of fluorine atoms) is narrower than line A. Its anisotropic shift is slightly negative and the value of its isotropic one is -109.75 ± 1 ppm. As opposed to line A, the orientational dependence of its linewidth roughly follows the rule $3\cos^2\Theta - 1$, meaning that the fluorinated molecules which give line B have a spinning motion around the c-axis, while line A corresponds to much less mobile molecules.

After removal of simulated lines A and B from the experimental spectra, a residual spectrum is obtained corresponding to $\sim 5\%$ of the fluorine atoms. At $\Theta = 0°$ and 90°, this residual spectrum is featureless, but at $\Theta = \Theta_m$, a relatively wide Gaussian line (C) is clearly visible ($\delta_0 = -111 \pm 1$ ppm).

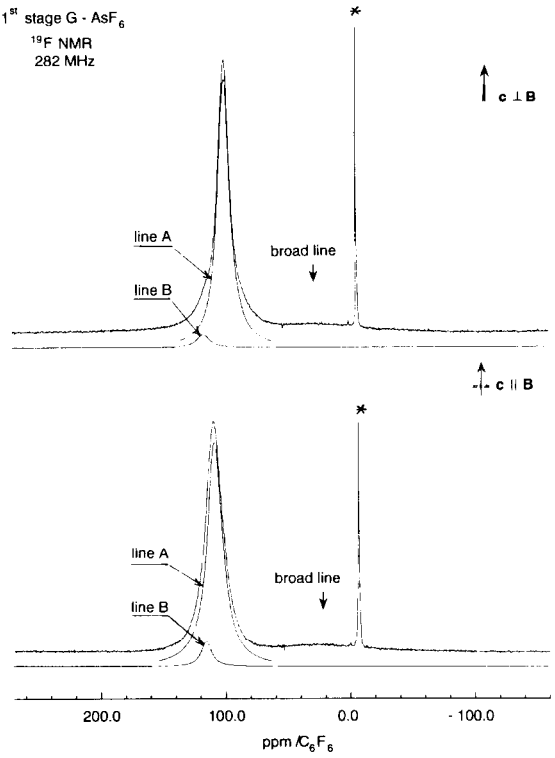

Fig. 2. ^{19}F NMR spectra at R. T. of first stage binary AsF_6–GIC at the two sample orientations $c \| B_0$ and $c \perp B_0$. The two simulated lorentzian lines A and B are also displayed. (The line marked * is due to SiF_4, resulting from the reaction of desorbed fluorine with glass, see text.)

The ^{19}F NMR spectra of the stage 1 arsenic fluoride graphite sample consist of a narrow line and a broad line (Fig. 2). The lineshape analysis of the narrow line shows that two lorentzian shape lines are present. The main line (A), which is representative of about 85% of all detected fluorine atoms, has orientation-dependent width and shift. The other line B ($\approx 5\%$ of the fluorine atoms) is narrower than line A If we assume that the lineshifts are axially symmetric around the c-axis, we can deduce both isotropic and anisotropic parts of the shift from the values measured at $\Theta = 0^\circ$ and $\Theta = 90^\circ$ for the two lines. The isotropic shifts are 103 ± 1 ppm and 116 ± 1 ppm, and the anisotropic shifts are $+9$ ppm and -1 ppm for lines A and B respectively. The broad line at ≈ 20 ppm is representative of $\sim 10\%$ of the fluorine atoms.

Discussion

Each of the lines observed in these two compounds is derived from specific fluorinated species, the identification of which can be made by comparing the isotropic lineshift to the ^{19}F chemical shift of various Group V fluorides. Both arsenic and antimony are known to given MF_3, MF_5 and MF_6^- fluorides, the chemical shifts of which are given in Table 3.

In the case of antimony fluoride GIC, it is clear from Table 3 that none of the lines can be attributed to SbF_3, and that line B is due to SbF_5. Moreover, since the isotropic shift of line A lies within the range of liquid $[SbF_6]^-$ shift values, we can attribute it to $[SbF_6]^-$, which means that antimony fluoride is preferentially intercalated as $[SbF_6]^-$ in this compound.

To identify fluorinated species giving line C in antimony fluoride GIC, we can consider fluoride polyanions $[Sb_n F_{5n+1}]^-$ which have been identified in liquid solution state on the basis of their ^{19}F NMR spectra [17]. These polyanions consist of *cis*-fluorine bridged polymeric structures where the fluorine atoms in axial positions labelled F_2 and F_5 by the authors are the most numerous. The corresponding lineshift depends on the solvent, but for a given solvent its value lies between the $[SbF_6]^-$ shift and the F_2 resonance in SbF_5 (*cf.* [17], Tables 1 and 3). More precisely, in SO_2ClF solution where the $[SbF_6]^-$ shift is -118 ppm, (the same as the isotropic shift value of line A in our GIC), the shifts of fluorine sites labelled F_2 or F_5 in polyanions lie between -108 and -113 ppm, compared with the shift of line C (111 ± 2 ppm). So we are led to attribute the line C to antimony fluoride polyanions.

The existence of such polyanions has been put forward to account for spectra observed in SbF_5–graphite [9]. But unlike the present observations, all of the spectra were attributed to polyanions, SbF_5 or $[SbF_6]^-$ being excluded.

In the case of arsenic fluoride GIC, we see from Table 3 that the isotropic shift of line A is almost the same as that of $[AsF_6]^-$ reported in [8]

TABLE 3

Chemical shifts (in ppm) of Group V fluorides, referred to $CFCl_3$ ($\delta_{C_6F_6} = \delta_{CFCl_3} + 163$ ppm)

	MF_3	MF_5	$[MF_6]^-$
M = Sb			
liquid state	−79 [7], −53.1 [8]	−108 [7], −109.6 [8], −111 [9], −112 [10]	−109.3 [8], −125 ≪ −117.9[a]
CIG			
G–SGF_5		−114 [12], −123 [13]	
G–AsF_5–NO_2SGF_6 [11]		−112.7	−124.1
our work		−110 (line B)	−118 (line A)
M = As			
liquid state	−42 [8], −40.4 [14]	−65.7 [8]	−58.9 [8], −69.5 [15]
CIG			
G–AsF_5 [16]		−52	
G–$AsF_5NO_2SGF_6$ [11]	−46.8	−66.7	
our work	−47 ± 1 (line B)		−60 ± 1 (line A)

[a]Depending on the solvent; data reported in [11].

(aqueous solution of $KAsF_6$). Thus we can identify arsenic fluoride giving this line as $[AsF_6]^-$. The isotropic shift of line B is nearer to an AsF_3 shift than to an AsF_5 one. It means that, unlike the antimony fluoride GIC, the arsenic fluoride GIC contains AsF_3 rather than AsF_5 as impurity.

Concerning the broad line, it is probably not due to any arsenic fluoride species. On the other hand, we might consider fluorine bonded to graphite carbon atoms. Indeed, such a broad line is observed at about -140 ppm in $(CF)_n$ compounds.

We conclude from the foregoing that, for both antimony and arsenic fluoride GICs prepared under fluorine atmospheres, fluorides are preferentially intercalated as $[MF_6]^-$. This method may lead to acceptor compounds having a charge transfer per intercalated molecule larger than in compounds prepared by other methods, where intercalated fluorides were a $MF_5/[MF_6]^-$ mixture.

^{19}F NMR spectra of metal fluoride/antimony fluoride compounds

Results

Like Group V fluoride GICs, metal fluoride/antimony fluoride GBCs exhibit ^{19}F NMR spectra resulting from the superimposition of several lines. The spectrum analysis at $\Theta = \Theta_m$ (Fig. 3) shows that, for both titanium and vanadium GBCs, the spectra consist of four lines, the characteristics of which are displayed in Table 4. The three lines A, B and C, which together represent about half of the observed fluorine atoms, are the same as the corresponding ones in antimony fluoride GIC, as can be seen from their chemical shift and width values. Therefore such lines are derived from antimony fluorides which have been intercalated in these GBCs. Since the lines A, B and C in binary antimony fluoride GIC have been attributed to $[SbF_6]^-$, SbF_5 and $[Sb_nF_{5n+1}]^-$ polyanions respectively, their relative areas give us information about the relative amounts of these species. Compared with binary antimony fluoride GIC, the amount of $[SbF_6]^-$ is lower in GBCs. In the case of vanadium GBC, this lowering is less, and is mainly to the benefit of SbF_5 species. In the case of titanium GBC, $[Sb_nF_{5n+1}]^-$ polyanions are heavily present at the expense of $[SbF_6]^-$ ions.

The characteristics of line D are the same in both titanium and vanadium GBCs. On the other hand, this line does not appear on the ^{19}F NMR spectra of binary second stage metal fluoride GICs we have recorded for comparison. This means that no intercalated metal fluoride was detected in GBCs.

The nature of the fluorinated species giving line D is not clear. We might suggest C bonded fluorine, though the shift of this line is different from those observed for the compounds $(CF)_n$ (≈ -145 ppm) and $(C_2F)_n$ (≈ -165 ppm) respectively.

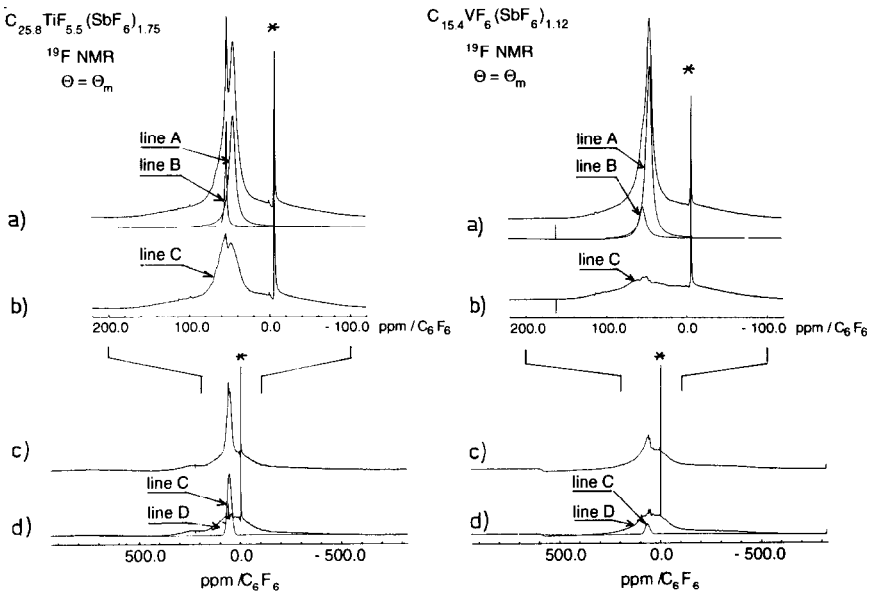

Fig. 3. The four lines of the ^{19}F NMR spectra at R. T. of metal fluoride/antimony fluoride GBCs. The sample orientation is (c, B_0) $\approx \Theta_m$. From the top to the bottom: a) experimental spectrum and simulated lines A and B; b) difference between experimental spectrum and simulated lines showing lines C and D; c) wider experimental spectrum after removing simulated lines A and B; d) simulated line C and difference between c) and line C showing line D. (The line marked * is due to SiF_4, resulting from the reaction of desorbed fluorine with glass, see text.)

TABLE 4

^{19}F NMR spectra of metal fluoride/antimony fluoride GBCs compared with binary antimony fluoride GIC

	G–TiF/SbF	G–VF/SbF	G–SbF
Line A	$\approx 17.5\%$	$\approx 35\%$	$\approx 88\%$
shift δ_0 (isotropic)[a]	−118 ppm	−117.75 ppm	−118 ppm
$\delta_\parallel - \delta_\perp$	+10 ppm	+12 ppm	+9 ppm
width	≈ 2.5 kHz	≈ 2.2 kHz	≈ 3.5 kHz
Line B	$\approx 5\%$	$\approx 10\%$	$\approx 5\%$
shift δ_0 (isotropic)[a]	−110 ppm	−111 ppm	−109.75 ppm
$\delta_\parallel - \delta_\perp$	−1 ppm		−3 ppm
width	< 1 kHz	≈ 4 kHz	≈ 1 kHz
Line C	$\approx 25\%$	$\approx 5\%$	$\approx 7\%$
shift δ_0 (isotropic)[a]	−112.5 ppm	−111 ppm	−111 ppm
width (at $\Theta = \Theta_m$)	7.35 kHz	7.5 kHz	4.6 kHz
Lind D	$\approx 52.5\%$	$\approx 50\%$	
shift δ_0 (isotropic)[a]	≈ -125 ppm	≈ -125 ppm	
width	≈ 50 kHz	≈ 50 kHz	

[a]From $CFCl_3$.

Discussion

The first point to discuss is why, in both titanium and vanadium GBCs, none of the lines of the ^{19}F NMR spectrum could be attributed to metal fluoride. First of all, it should be noted that, for the same amount of fluorine atoms, intercalated metal fluorides are much more difficult to detect than intercalated Group V fluorides. Indeed, the ^{19}F NMR spectra of binary second stage metal fluoride GICs lie over a very wide frequency range ($\approx$500 kHz), unlike those of Group V fluoride GICs ($\approx$15 kHz). Another possible explanation may be that subsequent intercalation of antimony fluoride could give rise to some chemical transformation of the intercalated metal fluorides. Whatever it may be, further investigation is needed to elucidate this point.

The second point to discuss is the high amount of $[Sb_nF_{5n+1}]^-$ polyanions encountered in titanium GBC alone. We think that it can be explained by the ability of titanium fluoride to form polyanions [18], unlike vanadium fluorides. Indeed, suppose that polymeric chains of titanium fluorides are formed according to the reaction:

$$[TiF_6]^- + (n-1)[TiF_5]^- \rightleftharpoons [Ti_nF_{5n+1}]^{(n+1)-}$$

The subsequent intercalation of antimony fluoride under fluorine pressure leads to intercalated $[SbF_6]^-$, which is able to break Ti_nF_{5n+1} chains according to the scheme:

$$[SbF_6]^- \rightleftharpoons SbF_5 + F^-$$

$$[Ti_nF_{5n+1}]^{(n+1)-} + F^- \longrightarrow [Ti_pF_{5p+1}]^{(p+1)-} + [Ti_qF_{5q+1}]^{(q+1)-}$$

$$(p+q=n)$$

The SbF_6^-/SbF_5 mixture obtained in this way is consistent with antimony fluoride polyanions.

Conclusion

The ^{19}F NMR spectra at room temperature of first stage binary Group V fluoride GICs prepared under a fluorine atmosphere show unambiguously that fluorides are intercalated preferentially as $[MF_6]^-$ species. Thus the charge transfer expected in these compounds is about one electron per intercalated fluorinated molecule. This charge transfer is higher than that observed in similar compounds prepared by other methods, where a value of about 1/3 per intercalated molecule is generally accepted [19].

In metal fluoride/antimony fluoride GBCs, the ^{19}F NMR spectra are consistent with antimony fluoride preferentially intercalated as $[SbF_6]^-$ in vanadium compounds, and as $[Sb_nF_{5n+1}]^-$ polyanions in titanium compounds. This latter result can be explained by the ability of titanium

fluoride to form polymer chains, unlike vanadium fluoride. No metal fluoride was observed. This could be due to the much lower sensitivity of ^{19}F NMR to these fluorides or their chemical transformation during antimony fluoride intercalation. Further investigations are needed to clarify this point.

References

1 T. Nakajima, K. Nakane, M. Kawaguchi and N. Watanabe, *Carbon, 25* (1987) 685.
2 T. Nakajima, T. Matsui, M. Motoyama and Y. Mizutani, *Carbon, 26* (1988) 831.
3 R. Yazami and T. Nakajima, *Synth. Met., 34* (1989) 109.
4 E. R. Falardeau, L. R. Hanlon and T. E. Thompson, *Inorg. Chem., 17* (1978) 301.
5 J. Melin and A. Herold, *C. R. Acad. Sci. Sér. C, 280* (1975) 641.
6 C. Meyer, R. Yazami, M. F. Quinton, A. P. Legrand and T. Nakajima, *Material Sciences Forum*, 1992, in press.
7 H. S. Gutowski and C. J. Hoffman, *J. Chem. Phys., 19* (1951) 1259.
8 E. L. Muetterties and W. D. Phillips, *J. Am. Chem. Soc., 81* (1959) 1084.
9 I. Stang, G. Roth, K. Lüders and H. J. Güntherodt, *Synth. Met., 12* (1985) 85.
10 C. J. Hoffman, B. E. Holder and W. L. Jolly, *J. Phys. Chem., 62* (1958) 364.
11 G. R. Miller, H. A. Resing, P. Brant, M. J. Moran, F. L. Vogel, T. C. Wu, D. Billaud and A. Proń, *Synth. Met., 2* (1980) 237.
12 G. Roth, K. Lüders and H. J. Güntherodt, *Synth. Met., 8* (1983) 91.
13 L. B. Ebert, A. R. Garcia and H. Selig, *Rev. Chim. Min., 23* (1986) 543.
14 J. K. Ruff and G. Paulett, *Inorg. Chem., 3* (1964) 998.
15 K. E. Christe, J. P. Guertin, A. E. Pavlath and W. Sawodny, *Inorg. Chem., 6* (1967) 533.
16 H. Sfihi, *Thèse de 3ème cycle*, Paris, 1983.
17 J. Bacon, P. A. W. Dean and R. J. Gillespie, *Can. J. Chem., 48* (1970) 3413.
18 E. Buscarlet, Ph. Touzain, M. Armand and L. Bonnetain, *C. R. Acad. Sci. Sér. C, 280* (1975) 1313.
19 J. Blinowski, H. H. Nguyen, C. Rigaux, J. P. Vieren, R. Le Toullec, G. Furdin, A. Herold and J. Melin, *J. Phys., 41* (1980) 47.